SolarPACES 2024, 30th International Conference on Concentrating Solar Power, Thermal, and Chemical Energy Systems

Solar Fuels and Chemical Commodities

https://doi.org/10.52825/solarpaces.v3i.2291

Published: 28 Nov. 2025

Development of a Concentrating Optics System for a Photoelectrochemical Hydrogen Reactor

SolarPACES 2024

A.W. Moelich[1], G.H. Creasey[2], J.W. Rodriguez-Acosta[2], A. Hankin[2], and C. McGregor[1]

[1]Stellenbosch University, South Africa

[2]Imperial College London, UK

*Correspondence: Craig McGregor, craigm@sun.ac.za

Abstract. Green hydrogen is expected to play a crucial role in achieving net-zero carbon emissions. By supporting the development of photoelectrochemical (PEC) hydrogen production, the technology's advantages in terms of scalability, low-cost materials, and reduced transmission losses can be utilised. This study presents the design, construction and characterisation of concentrating optics for on-sun testing with a PEC reactor. The optical design incorporates refractive primary optics (linear Fresnel lenses) and reflective secondary optics (stepped light-guide) to produce a scalable line-concentrating system. Ray tracing simulations predicted an optical concentration ratio (OCR) and optical efficiency of 12.5 and 51.3%, respectively. However, experimental testing revealed lower performance, with maximum OCR and optical efficiency of 5.8 and 23.8%, respectively. The greatest contributor to the discrepancy is found to be increased stray losses in the demonstrated system. While the optics were successfully coupled with a PEC reactor to produce hydrogen in subsequent on-sun tests, the high energetic losses limit its suitability for large-scale implementation. The results presented herein contribute to an extended study investigating the up scaling of PEC reactor technology.

Keywords: Concentrating Solar Optics, Linear Fresnel Lens Array, Solar Energy, Green Hydrogen, Photoelectrochemical Hydrogen Production

1. Introduction

1.1 Background

Due to its potential as an energy carrier, hydrogen is expected to play a crucial role in achieving net-zero carbon emissions. However, less than 0.7% of hydrogen produced in 2022 was produced using low-emission methods [1]. Therefore, if hydrogen's decarbonisation potential is to be realised, the production capacity of clean hydrogen must increase drastically.

One way to produce clean hydrogen is using a photoelectrochemical (PEC) hydrogen reactor that utilizes sunlight to drive the photoelectrochemical splitting of water into its constituents: hydrogen and oxygen. When compared to PV-electrolysis systems, PEC devices have advantages in terms of scalability, the use of low-cost materials, and a reduction in transmission losses [2]. However, the technology is still at an early developmental stage, with limited

studies reaching prototype-scale demonstrations [3]. Consequently, hydrogen produced using PEC technology is not yet economically feasible [2].

The high cost of photoelectrochemically produced hydrogen can be addressed by concentrating the sunlight incident on the reactor [4]. However, the concentration ratio should be limited to 100 and the output flux should be uniform to reduce accelerated degradation of the photo-absorbers in the PEC device [4], [5]. While current commercial solutions, such as parabolic troughs, can achieve the required concentration, they suffer from non-uniform output flux [6]. Therefore, an alternative solution - a system of lenses and lightguides - was considered in this study. Although reported optical efficiencies of lightguide systems are lower than that of parabolic troughs (50% to 70% [7], [8], and 80% [9], respectively), the concept was chosen for its ease of integration with an existing PEC reactor, as well as its increased flux uniformity.

1.2 Aim and Objectives

In a collaborative research effort, Stellenbosch University (SU) and Imperial College London (ICL) designed and built an up-scaled PEC reactor system which incorporates concentrating solar optics. The system was successfully demonstrated on SU's outdoor Solar Roof Laboratory. This research specifically addresses the development of the system's solar concentrating optical assembly, which incorporates a combination of refractive (linear Fresnel lenses) and reflective (polished aluminium lightguide) optical components to produce a scalable one-dimensional optical system for a prototype-scale PEC reactor.

2. Optical Design

To ensure successful coupling in future demonstrations, the optics had to meet additional requirements set by the reactor for which it was designed. The reactor had two photoactive components: a photoanode, located in the anodic half of the reactor behind a quartz window, and a photovoltaic cell, mounted externally on the opposite face of the reactor. Each photoactive area was 30 cm^2 in size, orientated in the vertical plane, and requiring lateral illumination from opposing directions. Along with these technical requirements, the optics were to be modular and equipped with dual-axis tracking. These requirements ensured on-sun testing in various configurations in future tests. The design also needed to allow the position of the optics to be manually fine-tuned to mitigate the effect of manufacturing errors.

2.1 Concept Design

The daylighting system proposed by Vu et al. [7] was used as a starting point for the design. Vu's concept used linear Fresnel lenses to collect and concentrate incident irradiance, and a stepped lightguide to direct the concentrated light from the lenses laterally towards its exit aperture. The lightguide irradiated a rectangular area in the vertical plane, complementing the shape of the photoanode aperture of the reactor. Additionally, since the concept concentrated light in only one dimension, it could be scaled easily by increasing its size in the direction of the horizontal dimension of the target. The dimensionality also meant that the large-scale application of the concept would only require single-axis tracking, as opposed to more expensive dual-axis tracking. The optical fibres shown in Figure 1 were discarded from the design presented in this study, since they were not required.

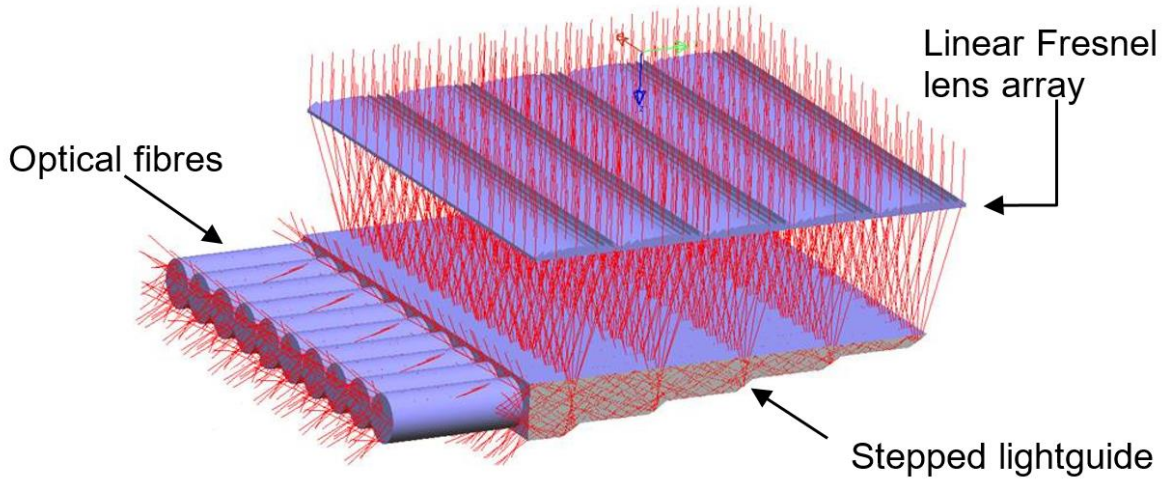

Figure 1. *Daylighting concept proposed by Vu et al. [7]. Diagram adapted from [7].*

To adapt the initial concept to the application of this study, several design changes were made. Firstly, the number of linear Fresnel lenses in the array was adjusted to three, according to the output flux required by the reactor. Using more lenses would collect more sunlight and ultimately result in a higher flux and optical concentration ratio at the exit aperture. Secondly, the proposed solid PMMA lightguide was replaced with a hollow, reflective lightguide. The new design was manufactured from Alanod Miro4® 4400GP, a specialised reflective aluminium sheet metal. Switching to a reflective lightguide reduced the attenuation losses within the light-guide and offered advantages in terms of local manufacturability.

The light path through the lenses and lightguide is shown schematically in Figure 2. The lenses were used to collect sunlight, concentrate it, and direct it into the reflective lightguide. The lightguide received the collected light and simultaneously homogenized and guided it laterally towards the reactor, ensuring a uniform distribution over the exit aperture. Two optical sub-assemblies (consisting of the linear Fresnel lens array and a corresponding lightguide) were used. The sub-assemblies were placed on either side of the reactor with the lightguides facing inward, producing concentrated sunlight on each of the two opposing photoactive areas of the PEC reactor.

Further refinements were made using design-level ray tracing simulations. The ray tracing studies were performed using the Ray Optics module in the COMSOL Multiphysics software package [10]. The geometry was simplified to a single optical sub-assembly. The simulation assumed ideal refraction through the linear Fresnel lenses but took into account transmission and reflection losses through the lenses and lightguide. Angular perturbations were also included to correct for the size of the solar disc.

Table 1 shows the categorisation of target surfaces for the irradiance transmitted through the system. The system achieved an optical efficiency of 51.3%, similar to the optical efficiency of 56.4% reported for the original refractive lightguide system proposed by Vu et al. [5]. The greatest contributor to optical losses (20.5% of the total input power) were stray losses. Stray losses occurred due to rays escaping the optical geometry without reaching the target surface. From the simulated ray trajectories, it was found that a large fraction of the rays entering the lightguide were reflected out through the entry apertures of the top surface. Other stray losses also occurred due to the angular perturbations introduced by the finite size of the solar disc. The stray rays can be seen in red in the ray trajectories plot in Figure 2. Although 225 000 rays were traced in the simulation, only 200 are shown in the figure. Rays that were incident on the target surface are shown in blue. Reflection losses and transmission losses refer to the energy

absorbed by the lightguide surfaces and linear Fresnel lenses, respectively. Combined, these losses make up the remainder of the energy losses in the simulation.

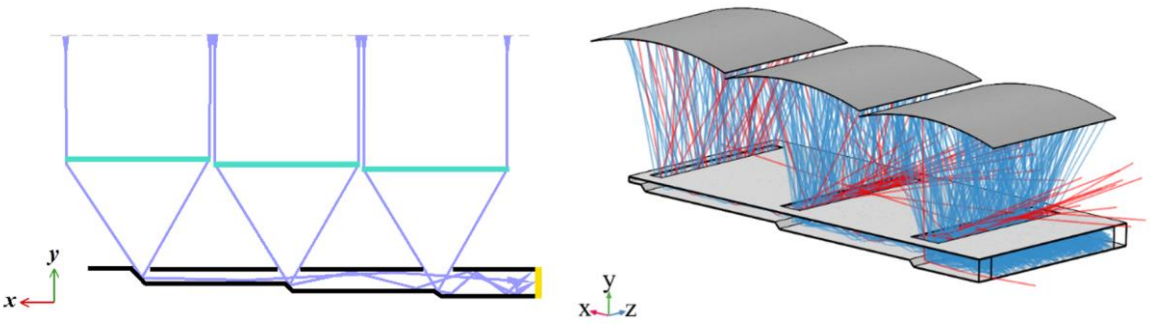

***Figure 2**. Left: Schematic representation of the ray path (light blue) through the linear Fresnel lenses (shown in cyan) and the lightguide (shown in black). The lightguide guides collected light laterally towards the photoactive components of the reactor (shown in yellow). Right: Simulated ray trajectories of a single lens-and-lightguide assembly. Rays incident on the target surface are shown in blue, while stray rays are shown in red.*

***Table 1**. Classification of simulated radiation energy fractions.*

Radiation energy fraction	Boundary	Simulated Result (% of input power)
Output power	Target surface	51.3
Stray losses	Bounding box	20.5
Reflection losses	Lightguide surfaces	20.2
Transmission losses	Linear Fresnel Lenses	8.00
	Total	100

Once the optical design was finalised, a supporting frame was developed to house the optical components. The support frame was modular, allowing the concentrating optical components to be exchanged with mirrors for reference testing of the reactor under non-concentrated irradiance conditions in future tests. The frame made use of slots at several bolted connection interfaces, allowing for the optical components to be adjusted in relation to each other. Therefore, manufacturing and assembly errors could be accommodated for by manually aligning the optical components until the system was “in-focus”. A diagram of the final design is shown in Figure 3. Post-design it was discovered that the optical surface of the linear Fresnel lenses did not match that of a plano-convex lens shape that would produce the focal length listed for the lens. Therefore, the optical surface, and consequently the optical output of the lens, differed from the simulated results.

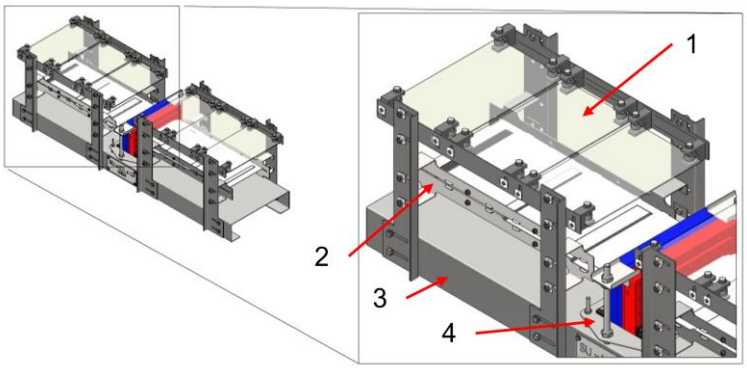

***Figure 3**. Annotated CAD diagram of the final design, showing the (1) lens array, (2) lightguide, (3) base, and (4) reactor mount with the reactor in blue and red.*

3. On-sun Demonstration

3.1 Experimental Design

Experimental testing took place on the Solar Roof Laboratory at Stellenbosch University (33.928 S, 18.865 E). The facility provided a dual-axis tracking platform, as well as global horizontal (GHI), direct normal (DNI), and diffuse horizontal (DHI) irradiance measurements. The solar data was measured with a Kipp & Zonen Solys2 solar tracker, equipped with a CHP1 pyrheliometer (DNI), shaded and unshaded CMP11 pyranometers (GHI and DHI) and a CM121 shadow ring with CMP6 pyranometer (DHI) [11]. Optical characterisation tests were performed in March 2024 to study the achieved optical concentration ratio (OCR), optical efficiency, spectral dependence and acceptance angle of the optical concept. On-sun demonstrations of the coupled optics-PEC system, in which hydrogen was produced, were performed in subsequent studies but are omitted here.

The flux output of the optics was measured by taking spectrometer readings at the exit apertures of each lightguide. Two spectrometers were used: A StellarNet BLACK-Comet UV-Vis measuring from 280 nm to 900 nm [12], and a StellerNet DWARF-Star Miniature NIR measuring from 900 nm to 1600 nm [13]. Readings were taken at three locations along the width of the lightguide exit aperture. The use of a cosine receptor ensured that all light in a 180° field of view was collected. An image of the experimental setup is shown in Figure 4.

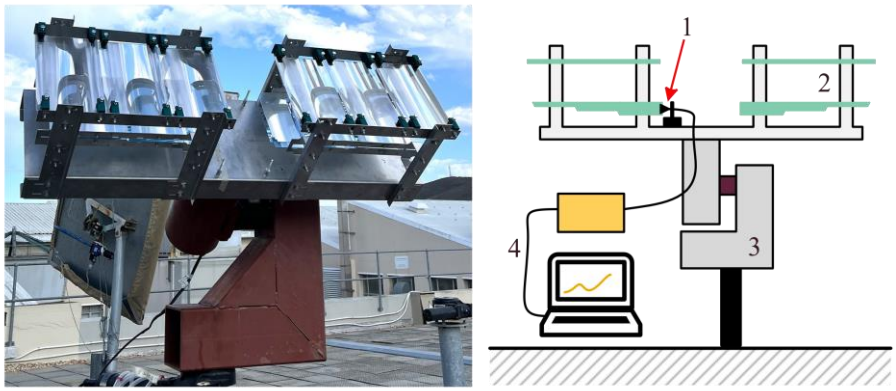

***Figure 4**. Image (left) and schematic (right) of the experimental setup, showing the (1) cosine receptor, (2) optics, and (3) dual-axis tracker, and (4) spectrometer and computer.*

3.2 Data Processing

To produce representative OCR and optical efficiency results using the spectrometer readings and measured solar resource, appropriate data processing steps had to be taken.

The DNI measured by the facility's solar station had to be corrected to represent the DNI over the wavelength ranges of the respective spectrometers. Using AM1.5G as a reference [14], the fraction of irradiance intensity in each wavelength range, f_{range}, was determined by integrating the spectral intensity, $i_{\text{AM1.5G}}(\lambda_j)$, over the wavelength range λ_{min} to λ_{max}, and dividing by the total intensity in AM1.5G, $I_{\text{AM1.5G}}$ [15]. Since the spectral data of AM1.5G is discrete, the equation is written more appropriately using summation notation:

$$f_{\text{range}} = \frac{1}{I_{\text{AM1.5G}}} \sum_{j=\lambda_{\text{min}}}^{\lambda_{\text{max}}} i_{\text{AM1.5G}}(\lambda_j) \Delta\lambda_j. \tag{3-1}$$

Consequently, the achieved OCR and optical efficiency, η_{optical}, could be calculated using equations 3-2 and 3-3, respectively, where $i_{\text{measured}}(\lambda_j)$ is the measured spectral intensity and GCR is the geometric concentration ratio of the optics [15]:

$$OCR = \frac{1}{f_{\text{range}}\, DNI} \sum_{j=\lambda_{\text{min}}}^{\lambda_{\text{max}}} \text{i}_{\text{measured}}(\lambda_j)\, \Delta\lambda_j, \tag{3-2}$$

$$\eta_{\text{optical}} = \frac{OCR}{GCR}. \tag{3-3}$$

The optics' acceptance angle was investigated by studying the change in optical performance relative to the incidence angle of the solar irradiance. To do this, the optical system was placed in the on-sun position, where it was assumed to have zero tracking error. The system was fixed in this reference position, and periodic spectral recordings of the optical output were taken as the sun followed its trajectory through the sky with passing time. The angle of incidence of the solar irradiance was determined from the azimuth and elevation angular displacements of the sun from the reference position.

4. Results

The results for the performance testing of the optical setup are presented and discussed in this section. **Table 2** shows a comparison of the simulated and experimentally achieved results. The experimental results showed significantly lower OCR and optical efficiencies than what was predicted with the ray tracing simulation. It is expected that the greatest contributor to the deviation from the simulated results is the non-ideal optical surface of the linear Fresnel lenses. As previously explained, the deviation from the surface of a plano-convex lens introduced undesirable defocusing of the concentrated light, likely leading to significantly increased stray losses. These stray losses also contributed to low achieved optical efficiency.

***Table 2**. Simulated and experimental optical performance results.*

Parameter	Symbol	Simulated Result	Achieved Result
Geometric concentration ratio	GCR	24.4	24.4
Maximum optical concentration ratio	OCR	12.5	5.8
Maximum optical efficiency	η_{optical}	51.2%	23.8%

The experimentally achieved OCR and optical efficiencies across multiple characterisation tests are plotted in Figure 5. Figure 5 also shows the dependence of the optical performance on the incidence angle of the irradiation.

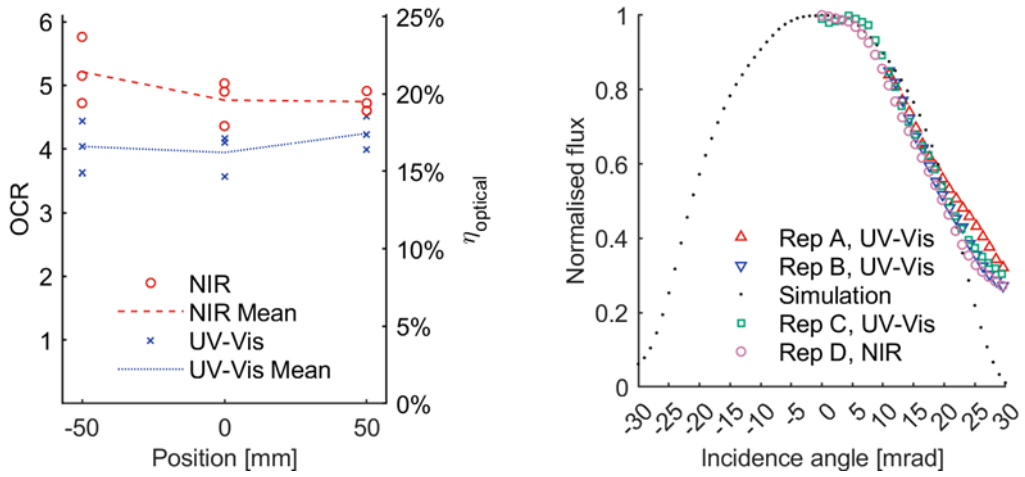

***Figure 5.** (Left) Experimentally achieved OCR and optical efficiencies across the width of the light-guide exit aperture. (Right) Optical performance versus incidence angle for repetitions A to D and the simulation.*

A clear separation between UV-Vis and NIR results is present in Figure 5, indicating a spectral response produced by the optics system. The reduced OCR in the UV-Vis range is due to absorption in the linear Fresnel lenses. Its material, Poly(methyl methacrylate) or PMMA, boasts a high transmission factor of 92%. However, investigating its spectral transmissivity reveals that the greatest absorption occurs at wavelengths between 200 nm and 380 nm [16]. Due to this absorption, less power in these wavelengths is transmitted through the lenses, to the lightguide and onto the exit aperture. The lower flux on the target surface consequently results in a lower OCR and optical efficiency at wavelengths in the UV-Vis range.

During the experimental study, it was found that the optics were sensitive to misalignment, as highlighted by the plot on the right of Figure 5. An acceptance angle of approximately 6 mrad, or 0.34°, exists for the optical system. However, further analysis showed that greater incidence angles significantly reduced the output flux on the target surface. At an angular displacement in the order of 10 mrad, the output flux decreased by nearly 20%.

Compared to competing one-dimensional concentrating solar optics in the literature, the optical efficiencies of 15% to 20% achieved in the experimental studies are low. Alternative technologies such as parabolic troughs have been demonstrated to achieve optical efficiencies in the order of 80% [9]. However, this number does not account for optical losses introduced when secondary optics are employed. The suggested optical system's performance could be improved by procuring more precise linear Fresnel lenses manufactured from materials that have higher transparency in the UV-vis region.

5. Conclusion

This work presents the development and characterisation of a solar concentrating optical system for use with a PEC reactor for hydrogen production. The system's modularity and use of horizontal lightguides ensured its successful coupling with a PEC reactor to produce hydrogen in subsequent studies. However, while the investigated optics suited the unique requirements of the existing PEC reactor, the relatively low maximum OCR and optical efficiencies of approximately 5.8 and 23.8% presented in this work suggests that the advantages gained with smooth system integration are negated by high energetic losses. The experimental work also highlighted the importance of precise optical components and control over tolerances in producing reliable and superior optical performance results.

Data availability statement

Data available upon request.

Author contributions

A.W. Moelich: Conceptualization, Formal Analysis, Investigation, Methodology, Project administration, Visualization, Writing – original draft, Writing – review & editing; **G.H. Creasey**: Investigation; **J.W. Rodriguez-Acosta**: Investigation; **A. Hankin**: Conceptualization, Investigation, Resources; and **C. McGregor**: Conceptualization, Funding acquisition, Investigation, Methodology, Resources, Supervision, Writing – review & editing.

Competing interests

The authors declare that they have no competing interests.

Funding

This work was supported financially by Stellenbosch University, GIZ, the South African Department of Science and Innovation, British Engineering and Physical Sciences Research Council (EPSRC) grant EP/W033216/1, and the Imperial College London 'Africa Strategic Partnership Fund', through student bursaries and the purchasing of equipment.

Acknowledgement

G. Creasey, J. Rodriguez-Acosta, and A. Hankin of the Electrochemical Systems Laboratory, Imperial College London, for the development, manufacturing, and operation of the PEC reactor.

References

[1] IEA, "Global Hydrogen Review 2023." (2024), [Online]. Available: https://www.iea.org/reports/global-hydrogen-review-2023 (visited on 04/30/2024).
[2] B. Moss, O. Babacan, A. Kafizas, and A. Hankin, "A Review of Inorganic Photoelectrode Developments and Reactor Scale-Up Challenges for Solar Hydrogen Production," *Advanced Energy Materials*, vol. 11, no. 13, p. 2003286, Apr. 2021. DOI: 10.1002/aenm.202003286.
[3] A. Vilanova, P. Dias, T. Lopes, and A. Mendes, "The route for commercial photoelectrochemical water splitting: a review of large-area devices and key upscaling challenges," *Chem. Soc. Rev.*, vol. 53, no. 5, pp. 2388–2434, Jan. 2024. DOI: 10.1039/D1CS01069G.
[4] B. A. Pinaud, J. D. Benck, L. C. Seitz, A. J. Forman, Z. Chen, T. G. Deutsch, B. D. James, K. N. Baum, G. N. Baum, S. Ardo, H. Wang, E. Miller, and T. F. Jaramillo, "Technical and economic feasibility of centralized facilities for solar hydrogen production via photocatalysis and photoelectrochemistry," *Energy Environ. Sci.*, vol. 6, no. 7, pp. 1983–2002, May 2013. DOI: 10.1039/c3ee40831k.
[5] O. Khaselev and J. A. Turner, "A Monolithic Photovoltaic-Photoelectrochemical Device for Hydrogen Production via Water Splitting," *Science*, vol. 280, no. 5362, pp. 425–427, Apr. 1998. DOI: 10.1126/science.280.5362.425.
[6] N. ur Rehman, M. Uzair, and M. Asif, "Evaluating the solar flux distribution uniformity factor for parabolic trough collectors," *Renewable Energy*, vol. 157, pp. 888–896, Sep. 2020. DOI: 10.1016/j.renene.2020.05.058.
[7] N. Vu and S. Shin, "A Large Scale Daylighting System Based on a Stepped Thickness Waveguide," *Energies*, vol. 9, no. 2, p. 71, Jan. 2016. DOI: 10.3390/en9020071.
[8] J. Lv, X. Xu, and P. Yin, "Design of leak-free sawtooth planar solar concentrator for daylighting system".
[9] P. D. Tagle-Salazar, K. D. P. Nigam, and C. I. Rivera-Solorio, "Parabolic trough solar collectors: A general overview of technology, industrial applications, energy market, modeling, and standards," *Green Processing and Synthesis*, vol. 9, no. 1, pp. 595–649, Nov. 2020. DOI: 10.1515/gps-2020-0059.
[10] COMSOL, "Ray Optics Module." (2024), [Online]. Available: https://www.comsol.com/ray-optics-module (visited on 08/21/2024).
[11] Kipp & Zonen, "Solar Instruments." (2024), [Online]. Available: https://www.kippzonen.com/ProductGroup/1/Solar-Instruments (visited on 08/21/2024).
[12] StellarNet, Inc., "BLACK-Comet UV-VIS Spectrometer." (2024), [Online]. Available: https://www.stellarnet.us/spectrometers/black-comet-uv-vis-concave-grating-spectrometers/ (visited on 08/21/2024).
[13] StellarNet, Inc., "DWARF-Star Miniature NIR Spectrometer." (2024), [Online]. Available: https://www.stellarnet.us/spectrometers/dwarf-star-miniature-nir-spectrometer/ (visited on 08/21/2024).

[14] NREL, “Reference Air Mass 1.5 Spectra.” (2004), [Online]. Available: https://www.nrel.gov/grid/solar-resource/spectra-am1.5.html (visited on 08/21/2024).
[15] J. Hogerwaard, I. Dincer, and G. F. Naterer, “Experimental investigation and optimization of integrated photovoltaic and photoelectrochemical hydrogen generation,” *Energy Conversion and Management*, vol. 207, p. 112541, Mar. 2020. DOI: 10.1016/j.enconman.2020.112541.
[16] P. Thi Hong, H. Q. Nguyen, and H. T. M. Nghiem, “Complex refractive index measurements of poly(methyl methacrylate) (PMMA) over the UV-VIS-NIR region,” *Opt. Continuum*, vol. 2, no. 11, p. 2280, Nov. 2023. DOI: 10.1364/OPTCON.495634.